Estimation of Needle Tissue Interaction based on Non-linear Elastic Modulus and Friction Force Patterns *

Inko Elgezua*, Yo Kobayashi, member IEEE, and Masakatsu G. Fujie, *Fellow IEEE*

Abstract— **Incidence of cancer is growing worldwide according to statistics, what increments costs of national health systems and decreases quality of life of cancer patients. Percutaneous cancer treatments can reduce the physical burden of cancer patients due to its minimally invasiveness and allow to treat small size tumors. Robotic needle placement has been proposed to overcome the difficulties of manual needle placement, which has not enough accuracy. Until now, researchers have focused on developing deterministic models for pre or intra-operative control. In this paper, we propose a novel approach by extracting patterns in needle insertion force that can provide information about the current status of needle tissue interaction. In particular, we focus in estimating the non-linear local elastic modulus and friction status in real-time during needle insertion.**

I. Introduction

According to statistics of the World Health Organization, in the year 2012 there were 14.1 million new cancer cases worldwide with another 32.6 million already diagnosed [1]. This not only creates an economical impact on national health systems, but more importantly, it imposes a big psychological and physical burden on cancer patients, who often must endure the serious side effects of chemo- and radiotherapy.

Since the introduction of laparoscopic surgery, patients and hospitals are benefiting from the advantages of minimally invasive surgery (MIS): better cosmetic outcomes, less trauma, reduced number of post-operatory complications and shorter hospitalization. Not surprisingly, physicians have also shown interest in MI interventions for cancer patients.

For example, by the year 2007 more than 1500 centers provided radio frequency ablation (RFA) for liver cancer in Japan, and it has become and accepted alternative to open surgery for small size cancers [2]. RFA is a type of percutaneous intervention, that are those that access internal organs through the skin, commonly with the use of needles. Other percutaneous cancer interventions include cryoablation, chemotherapy, brachytherapy and biopsy.

Percutaneous interventions are a difficult task for physicians. Human tissue is soft and easily deformable when the needle is introduced, what causes the target to move. Involuntary patients' movement, such as respiration, and needle bending are also factors that contribute to errors in needle placement. With reduced visibility due to the limitations of medical imaging and low needle maneuverability, manual needle placement error is found to be 3 to 5 mm [3][4]. Considering that the maximum recommended cancer size for RFA application is 30 mm [5], with even targets as small as 5 mm [6], in the best-case scenario the error mentioned above yields a 20% needle placement error from the tumor's center.

To overcome the limitations of manual needle insertion, use of robotic systems have been proposed. Aiming robots can hold and orientate surgical tools in complex three-dimensional poses that are difficult to achieve by hand, but as the needle is inserted manually, the problems of tissue deformation, needle bending and patient's movement are not solved.

Kobayashi *et al.* [7] and DiMaio *et al.* [8] proposed to use Finite Elements (FE) simulation to estimate how the tissue is going to deform and calculate a needle trajectory that will hit the target. Although they can achieve good results, under 2 mm error, FE simulations require precise knowledge of the values of biomechanical parameters, which present a big variation between person to person and are difficult to measure non-invasively. Furthermore, because FE simulations are computationally expensive, it is not suitable for intra-operative control.

Needle steering with ultrasound (US) image has also been proposed [9] but it has been validated only in artificial phantom tissue that provides a less noisy image. Needle and target tracking are still open problems in real tissue. Since Webster *et al.* [10] first proposed flexible needles to steer a needle into a desired path, research in this area has become popular [11-15].

Planning and control of flexible needles have provided interesting results, but most of these proposals have been validated with artificial phantom tissue, or assume deterministic models. But, needle tissue interaction presents a complex behavior and variations that cannot be modeled deterministically.

In this paper we propose a novel approach to the problem of needle insertion. We aim to estimate the needle tissue interaction status by means of the estimated local value of non-linear elastic modulus and friction force. In the next section we introduce the concept of situation awareness for surgical robots and the importance of adapting and reacting to changing or unexpected conditions. From section IV onwards the technical details of puncture detection, friction and non-linear modulus estimation and associated needle tissue interaction patterns are presented.

Inko Elgezua and Yo Kobayashi are with the Graduate School of Advanced Science and Engineering, Waseda University. TWIns, 03C201, Wakamatsu-cho, Shinjuku, Tokyo, Japan; 162-8480 (phone/fax: +81 3-5369-7330; e-mail: ielgezua@ asagi.waseda.jp.

Masakatsu G. Fujie is with the Faculty of Science and Engineering, Waseda University, Japan.

II. Situation Awareness Percutaneous Robot

A. The steerability of rigid needles is inversely proportional to the insertion depth, and flexible needles have a limited bending radius. This means, that they cannot reach any point located in a circle tangent to the tip of the needle and whose radius equals the needle's curvature radius [15]. Therefore, due to the underactuated nature of needles into soft tissue, it is necessary to predict in advance the future position of the target in order to calculate a path that can reach it.

Typically, needle insertion simulators assume a constant pattern of tissue deformation, puncture and tissue relaxation. But analysis of real insertion force shows that this is rarely the case. Living tissue is inhomogeneous, non-linear and viscoelastic. Although in general the steady cutting pattern described above is common, often there are also situations with abrupt tissue rupture, vein or membranes puncture or needle sliding that alter the way in which tissue deforms. Furthermore, there can be unexpected situations that a robot must react to. It is common when performing needle insertion into porcine breast tissue to find ligaments in the needle path, which is much harder to puncture than the surrounding mammary gland, and the needle simply deforms the tissue without advancing into it. This is far from anecdotic evidence. Other research teams have also reported needle buckling when experimenting with porcine liver [15].

Standard needle insertion robots have as inputs insertion force and medical imaging to simulate how the tissue will deform, or just calculate a trajectory, but it has been recognized by many researchers that intelligent intra-operative control is needed to adapt to dynamic environments. Our future goal is to create such a percutaneous robot. For this reason, we propose the inclusion of a situation awareness module (Fig. 1), which can be defined as *the ability to perceive the environment in a given time and space, understand its meaning, and predict a new status when variables change*. The ultimate goal is to extract information from the measured insertion force for decision-making. In other words, we aim to imitate the ability of physicians' hands to feel the environment and react to it.

In [16] we addressed the problem of identifying the type of tissue being punctured. The goal was to detect transition between states when a needle insertion is modeled as a finite state machine. In this paper we focus only on identifying those patterns that can indicate needle-tissue interaction status and can affect how tissue will deform. This is another step towards the development of a full situation awareness system.

III. Experimental Data Used for Validation

The data used to validate the proposed method has been collected from *ex-vivo* porcine liver. Unless otherwise indicated, each example in this paper corresponds to different livers and insertion speeds in order to prove the generality of the proposed method.

All proposed algorithms have been validated with the data acquired with the following setup: A series of needle insertions in five different porcine livers were carried out with an 18G–1 1/2" surgical needle. The lobes of each liver were dissected and each lobe was used for experimentation. Each lobe was put on a flat metallic surface to ensure similar
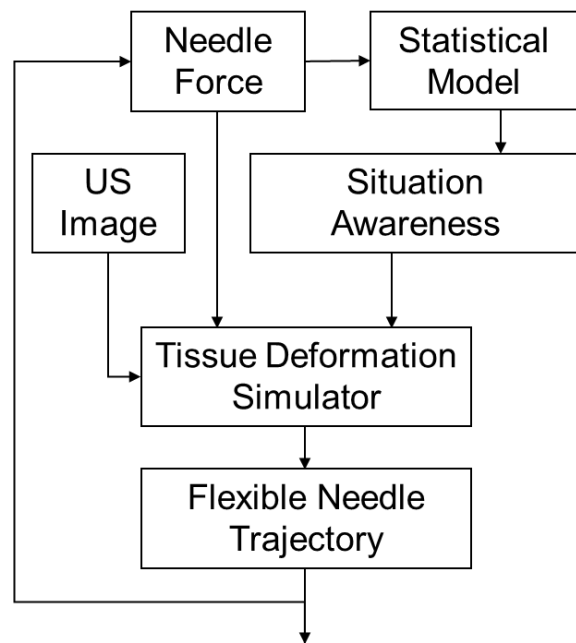

Figure 1. Diagram of the proposed situation awareness system. The present work focus only in the situation awareness problem.

boundary conditions. A needle was inserted vertically using a Cartesian robot (Fig. 2). The punctures were distributed in a matrix like pattern with each row and column equally separated 5 mm from each other.

The needle was inserted 15 to 30 mm deep depending on the liver thickness. The number of punctures varies from 75 to 250 depending on the liver size (both adult and young porcine livers were used). The needle insertion force was recorded with a sampled rate of 1 kHz using a 6-axis Nano force sensor by BL Autotech (max. load force 5 N ± 1.5% and resolution of 10 mN in the axial direction).

Because of viscoelastic behavior of living tissue, the needle insertion speed was randomly selected from 0.75 mm/s to 6 mm/s with increments of 0.75 mm/s for a total of 8 different insertion speeds. For each insertion speed the same number of punctures was performed in each lobe.
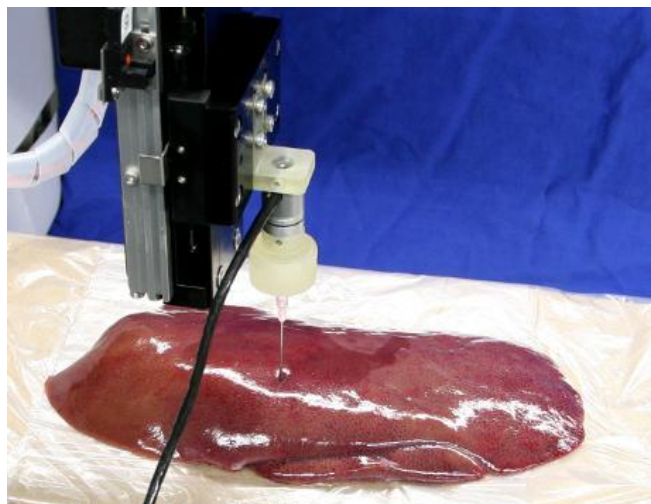

Figure 2 Experimental setup for force pattern identification of liver puncture.

IV. REAL-TIME PUNCTURE DETECTION

When a needle is inserted into soft tissue, first it will push the tissue deforming it, when the stress limit is reached it will puncture the tissue and advance into it while tissue relaxes. This is called the cutting force and it is only applied to the tip of the needle. The puncture or rupture event can be easily seen in a needle insertion force against needle position as a sharp drop in force. This drop happens when the tissue ruptures and the force in the tip of the needle disappears. At that moment friction between the surface of the needle and surface of the needle becomes the dominant force, which is smaller than the puncture force. As a result a characteristic saw profile is generated. In general, needle insertion force has two components:

$$F_{Tip} = F_{Cutting} + F_{Friction} \qquad (1)$$

this model was first proposed by Okamura *et al.* [17]. In their experiment with porcine liver, they also included a term for the puncture of the membrane that covers the liver, however this is a special case in which friction force is zero.

Friction force is due to the interaction of tissue with the surface of the body of the needle, it is always bigger or equal to zero and proportional to the needle position into the tissue. On the other hand, cutting forces increase steadily until the tissue breaks and the cutting force disappears abruptly. This pattern generates a triangular shape. Both forces combined produce a saw profile (cutting forces) overlapped to the general increasing trend due to friction force (Fig. 3).

Several methods have been proposed to detect tissue puncture in real-time. For example Washio *et al.* [18] used a special device that covered the needle, except the tip, with a sheath connected to a second force sensor. In this way, cutting force and friction were separated.

Barbé *et al.* [19] used a rheological model to fit the insertion force using recursive least square method. Then used fault detection algorithm to detect sudden changes in the value of the parameters in their model. Their approach produced fast puncture detection but it requires the use of a fitting model, which might not be always the case, for example when only puncture force is needed.

Instead, we propose a general puncture detection algorithm that it is model independent and doesn't require special hardware. As explained earlier, cutting force has a triangular shape. Ideally, if the sampled force has no noise, when the last sampled point, x_n, is smaller than the previous point x_{n-1}, it would indicated a decrease of force meaning a puncture has occurred. However, real signals are affected by noise, what makes the condition $x_n - x_{n-1} < 0$ possible even if the general trend is increasing. Therefore, the naive approach described above is not feasible in practice.

Given the sampling rate of 1 kHz and the relative slow changing speed of needle insertion force, the variation between consecutive points $x_n - x_{n-1}$ is constrained (Fig. 4) regardless the needle insertion force pattern. Furthermore, the measured difference between consecutive sampled points follows a normal distribution.

In order to detect puncture events, the proposed algorithm keeps an array of the last k-sampled points. For each new sampled force the procedure is as follows:

1. Remove first point of the array. Add the last point to the kth position.

2. Update standard deviation σ of differences of consecutive points with $x_k - x_{k-1}$.

3. Find the maximum value (x_{max}) of the array.

4. If the condition $x_{max} - x_k > 6\sigma$ is true, a puncture is detected.

For best results the value k has been set experimentally to 100. When a new point is sampled, to remove high-frequency noise, the signal it is filtered with a moving average filter of the last 5 points. It must be noted that the expected value between two points with the differences normally is given by:

$$\Delta x_{m-n} = (m - n)\mu_s + \sqrt{m - n}\sigma_s \qquad (2)$$

Where μ_s and σ_s are the mean and standard deviation of the increments of consecutive points. This is different than the rule given in the fourth point of the algorithm process. The reason is that we are not interested on detecting whether the difference between two points differs from the expected difference, but to find when the difference between those points cannot be explained only by signal noise.
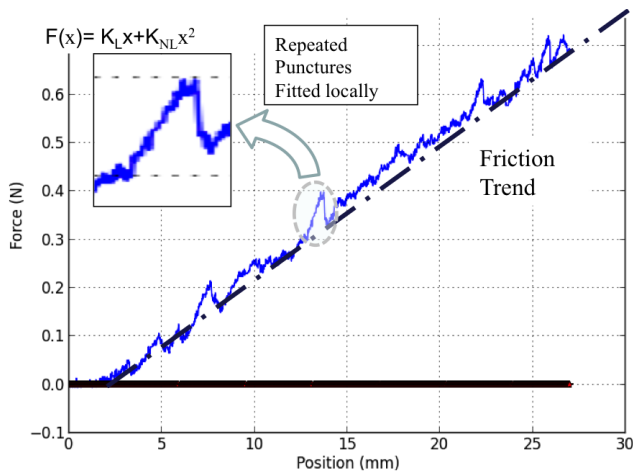

Figure 3 Friction force produces a general trend that it is proportional to needle depth. Cutting forces have a triangular shape that overlaps with friction producing the characteristic profile of needle insertion force.
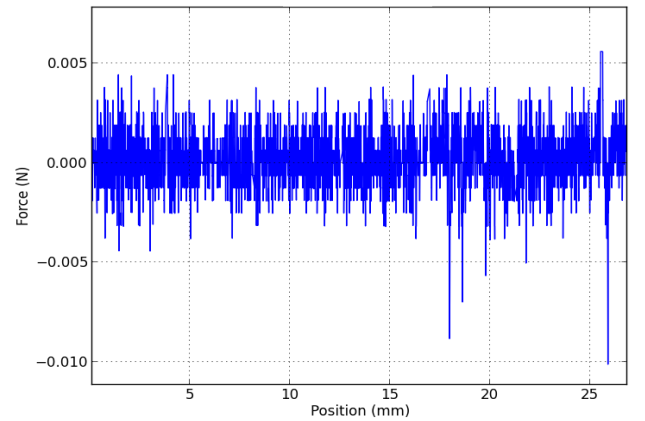

Figure 4 Differences between consecutive sampled points $x_n - x_{n-1}$ for a randomly chosen insertion. It can be seen that the variation is constrained to a band between $\pm5\text{x}10^{-3}$ N.

Until the puncture occurs, the measured force in the tip must increase, thus, the maximum point must be always the last sampled point. However, due to noise it is possible that this is not the case, but if it is due only to noise, the following sampled points eventually must become greater than the previous ones since the force is increasing. If the difference between the maximum value found and the last sampled points continue increasing, this is cannot be explained by noise alone, but a puncture event that decreases tip's force must have occurred.

To increase the robustness and tolerance to noise of the proposed puncture detection algorithm, we took as threshold the value of 6σ. According to the properties of the normal distribution, only 2 in a billion of randomly selected values from the given distribution will be at a bigger distance of μ±6σ.

After a puncture is detected, the end of the relaxation phase is also detected. After the tissue relaxes, the force on the tip of the needle starts to increase again, this moment is found with the same method proposed to find a puncture event but instead of the maximum point, now the minimum is used.

The proposed puncture detection algorithm was validated with force measurements taken from 5 different *ex-vivo* porcine livers. The detection accuracy is estimated with 15 randomly selected needle insertions out of 400 (around 100 puncture events in total). Experimental results show a detection accuracy approximately of 95%, commonly very small punctures are not detected. The average puncture detection time is 42.1 milliseconds, standard deviation 27.3, and a maximum and minimum detection time of 100 and 4 milliseconds respectively. Fig. 5 shows two examples of puncture detection. A red starts marks when the puncture occurs, a green start the end of the relaxation phase and beginning of a new cycle of pushing-puncturing.

V. CUTTING AND FRICTION FORCE MODELS

According to (1), the force measured on the needle has two components: cutting force and friction force. Cutting force depends on the type of tissue, needle's tip shape and size. Commonly, it is considered that also depends on the insertion speed because of viscoelastic property of living tissue. However, in [16] we proved that in practice this is not the case. It influences how much tissue deforms before breaking, but puncture force has big enough variation that no statistical difference is found between different insertion speeds. However, friction presents a much complex behavior that it is not yet fully understood.

Although cutting and friction forces should be estimated in parallel, this is difficult to achieve due to the existence of multiple solutions. As a first step in order to detect patterns and relations between cutting and friction forces, we will assume that the force measured during the deformation phase is only cutting force, fit locally a quadratic model to estimate the non-linear elastic modulus, and after a puncture occurs and tissue relax, we fit a linear model of friction. Then, the cutting force can then be recalculated as the difference between measured force and estimated friction force.

Instead of using a unique model to fit all the points, we use a simple model that it is fitted locally. A quadratic model has been found to fit better the small deformations and forces involved. A quadratic model was also proposed in [18], but without physical interpretation:

$$F_{Cutting} = K_{kL}(x - x_{k0}) + K_{kNL}(x - x_{k0})^2 \qquad (3)$$

where x is the needle position, x_{k0} is the position at which the kth puncture starts, and K_{kL} and K_{kNL} are the linear and non-linear elastic modulus for the kth puncture. The value of x_{k0} is found with the algorithm described in the previous section, and the model is fitted using least squares method for the new measured force until a puncture is detected. At that
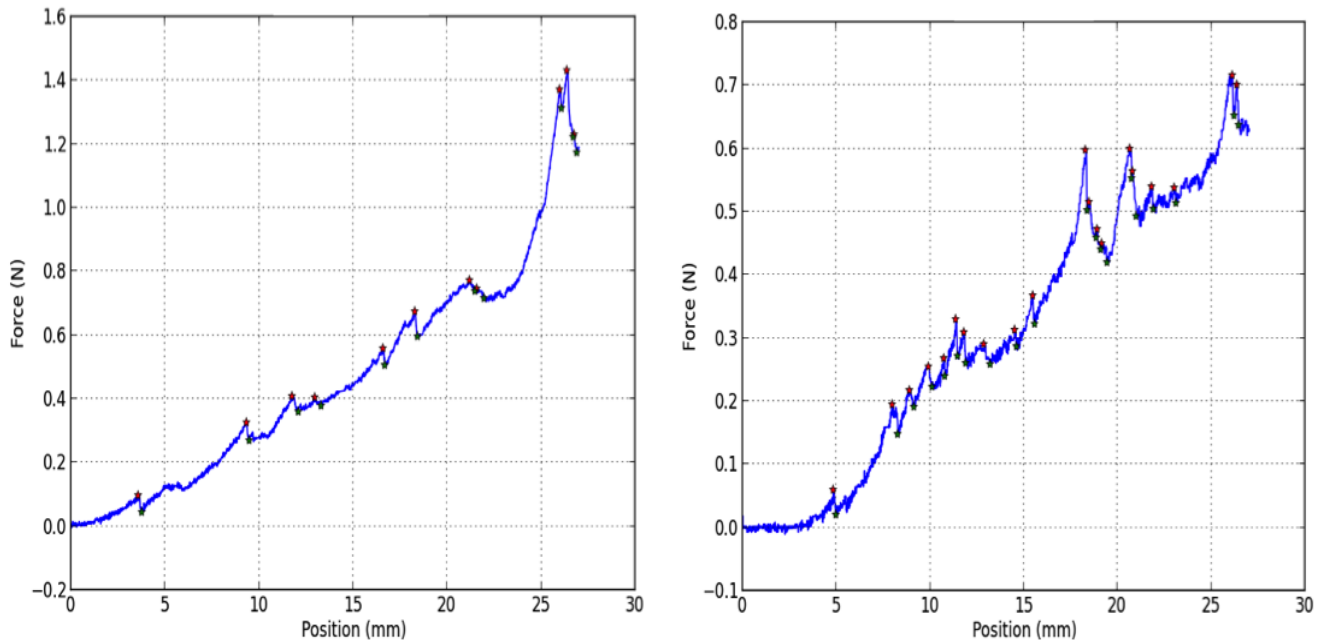

Figure 5 Examples of puncture detection with the proposed algorithm. Red starts indicate puncture detection and green beginning of the next cycle.

moment the fitting stops until the tissue finish to relax and a new puncture begins.

The proposed model is validated using the same data from *ex-vivo* porcine liver with which the puncture detection algorithm was validated. Results show commonly a correlation factor of $R^2 \geq 0.9$. There are however instances when the parameter K_{kNL} becomes negative. Since this has no physical meaning, despite a better fit, in those instances the non-linear parameter is set to zero and a simple linear model is used instead.

Friction modeling for needle insertion has an extensive literature. Perhaps, one of the most complete is the proposal by Asadian *et al.* [20] of a modeling scheme using iterative Kalman filters to fit a LuGre model, because it allows to determine stick-slip conditions between tissue and needle. However, their approach, although it provides a good fit, it is unrealistic because it assumes that the only cause of the force acting on the needle is friction, which is not true [17]. The authors themselves acknowledge the lack of physical meaning of the parameters of the model.

Standard friction models are unnecessarily complicated to detect stick-slip conditions in needle insertion. Instead, a linear model can be used locally to determine stick-slip conditions. After the tissue is punctured, it relaxes and the force measured on the needle decreases. Due to friction and remaining stress on tissue, the residual force after puncturing is not zero. However, because of the small increments of friction force after each puncture and small deformations involved, a linear model can be fitted locally for each individual puncture:

$$F_{Friction} = \frac{F_{k\,min} - F_{k0}}{x_{k0} - x_{k\,min}}(x - x_{k0}) \qquad (4)$$

where $F_{k\,min}$ is the force measured after the tissue finishes relaxing (or the next puncture starts), F_{k0} is the force when the kth puncture begins, and x_{k0} and $x_{k\,min}$ are the needle positions when the kth puncture starts and ends respectively. Similarly to the local fitting, the parameters necessary to fit the model are calculated from the points detected by the puncture detection algorithm. Fig. 6 shows four examples of the linear model locally fitted to measured insertion force into *ex-vivo* porcine liver. Each of the graphs corresponds to a different needle insertion speed.

As can be seen, the proposed locally fitted linear model can follow the shape of the insertion force no matter its profile. It has to be mentioned however, that for the first puncture there is no component of friction. This is simply because the needle is still entirely outside the tissue. For that reason we only fit the friction model once the initial puncture is detected.

Analysis of the different elastic-modulus and friction patterns (slope of each segment) for more than 400 insertions into ex-vivo porcine liver show four different situations:

- Steady cutting and friction forces
- Vein puncture
- Tissue-needle sliding
- Decrease in insertion force

The first pattern is characterized by linear friction force with little variation in friction slope and non-linear elastic modulus coefficients (top left graph in Fig. 6). Vein puncture is associated with higher values of elastic modulus and friction (top right graph at 19 mm). Slip condition appears often after a puncture and is typically less than 1 mm (Fig. 6 bottom left graph between 15 and 16 mm, and top left at 22 mm). The principal characteristic is a slope value of friction near zero. A possible explanation of this effect could be related to crack propagation before tissue stops sliding over the needle after rupture, but experimental evidence is needed to support this hypothesis.

Finally, sudden decreases in insertion force have also been observed. Although it happens frequently, the average width is 0.5 mm. The case shown at the bottom right graph of Fig. 6 is an extreme case. The cause of this sudden decrease is not well understood and more work is needed to explain the causes, which could be related to slippage or abrupt tissue rupture due to residual stress.

VI. Conclusion

We introduced a novel approach to percutaneous interventions with the introduction of the situation awareness concept, and justified the need for it in percutaneous robots.

Next, we proposed a puncture detection algorithm, which shows good experimental results with a puncture detection rate of 95%, and an average detection time of 42.1 milliseconds. For the application of needle insertion this detection time is considered adequate. However, the algorithm needs to be improved to detect small punctures.

Finally, we proposed the use of a quadratic model to fit locally the value of the non-linear elastic modulus and a linear model for friction. Experimental results show that both models fit well the data and can follow the changing trends of insertion force. However, vein puncture presents often a double peak shape. The current version of the friction fitting model doesn't takes into account this situation and calculates higher values of friction because it take the force value before tissue relaxation after vein puncture.

Analysis of elastic modulus and friction allowed us to identify four distinctive patterns: steady tissue cutting, vein puncture, slip and sudden decrease in insertion force.

The proposed methods in this work can determine past situations: puncture, tissue slip, etc. but as explained in section II, it is also necessary to predict future events, for that reason in future work we aim to develop an algorithm that can estimate the future profile of needle insertion force based on past values of friction and cutting forces. This estimated profiles could be used then in a real-time tissue deformation simulator in order to predict the final position of a target and estimate a needle trajectory in real-time.

References

[1] International Agency for Cancer Research, World Health Organization, "Globocan 2012: Cancer Fact Sheets" http://globocan.iarc.fr/Pages/fact_sheets_cancer.aspx.

[2] S. Shiina, "Japanese experience in ablation therapies for hepatocellular carcinoma," Hepatol Res., Sep 2007, 37 Suppl 2:S223-9.

[3] E.M. Boctor, M.A. Choti, E.C. Burdette, R.J. Webster, "Three-dimensional ultrasound-guided robotic needle placement: An experimental evaluation," Int. J. Med. Robot. Comput. Assist. Surg., vol. 4, no. 2, pp. 180–191, 2008.

[4] L. Maier-Hein, F. Pianka, A. Seitel, S.A. Müller, A. Tekbas, M. Seitel, I. Wolf, B.M. Schmied, H.P. Meinzer, "In vivo accuracy assessment of a needle-based navigation system for CT-guided radiofrequency ablation of the liver", Medical Physics, 35, 5385-5396, 2008.

[5] P. Abitabile, U. Hartl, J. Lange, C.A. Maurer, "Radiofrequency ablation permits an effective treatment for colorectal liver metastasis", European Journal of Surgical Oncology (EJSO), vol. 33, Issue 1, pp. 67-91, 2007.

[6] S. Oura, T. Tamaki, I. Hirai, T. Yoshimasu, F. Ohta, R. Nakamura, Y. Okamura, "Radiofrequency ablation therapy in patients with breast cancers two centimeters or less in size", Breast cancer, p. 48-54, 2007.

[7] Y. Kobayashi, J. Okamoto, M. G. Fujie, "Physical Properties of the Liver and the Development of an Intelligent Manipulator for Needle Insertion," Robotics and Automation (ICRA), vol., no., pp.1632-1639, 18-22 April 2005

[8] S.P. DiMaio, S.E. Salcudean, "Interactive simulation of needle insertion models," Biomedical Engineering, IEEE Transactions on , vol.52, no.7, pp.1167-1179, July 2005.

[9] D. Glozman, M. Shoham, "Image-Guided Robotic Flexible Needle Steering," Robotics, IEEE Transactions on , vol.23, no.3, pp.459-467, June 2007.

[10] R.J. Webster III, J. Kim, N. Cowan, G. Chirikjian, A. Okamura, "Nonholonomic Modeling of Needle Steering," The International Journal of Robotics Research, vol. 25 no. 5-6, pp. 590-525, May-June 2006

[11] R. Alterovitz, M. Branicky, K. Goldberg, "Motion Planning Under Uncertainty for Image-Guided Medical Needle Steering," The International Journal of Robotics Research, vol. 27, no. 11-12, pp. 1361-1374, November/December 2008

[12] S.Misra, K.Reed,B. Schafer, K.Ramesh, and A.M.Okamura, "Mechanics of flexible needles robotically steered through soft tissue," Int. J. Robot. Res., vol. 29, pp. 1640–1660, 2010.

[13] N.A Wood, K. Shahrour, M.C. Ost, C.N. Riviere, "Needle steering system using duty-cycled rotation for percutaneous kidney access," Engineering in Medicine and Biology Society (EMBC), pp.5432-5435, September 2010.

[14] M.C. Bernardes,B.V. Adorno, P. Poignet, N. Zemiti, G.A. Borges, "Adaptive path planning for steerable needles using duty-cycling," Intelligent Robots and Systems (IROS), pp.2545-2550, Sept. 2011

[15] D.C. Rucker, J. Das, H.B. Gilbert, P.J. Swaney, M.I. Miga, N. Sarkar, R.J. Webster, "Sliding Mode Control of Steerable Needles," Robotics, IEEE Transactions on , vol.29, no.5, pp.1289,1299, Oct. 2013.

[16] I. Elgezua, S. Song, Y. Kobayashi, M. G. Fujie, "Event Classification in Percutaneous Treatments based on Needle Insertion Force Pattern Analysis", The International Conference on Control, Automation and Systems, ICCAS. Gwangju, Korea, October 20-22 2013.

[17] A.M. Okamura, C. Simone, M.D. O'Leary, "Force modeling for needle insertion into soft tissue," Biomedical Engineering, IEEE Transactions on , vol.51, no.10, pp.1707-1716, Oct. 2004.

[18] T. Washio, K. Chinzei, "Needle force sensor, robust and sensitive detection of the instant of needle puncture," Medical Image Computing and Computer-Assisted Intervention, vol. 3217, pp. 113-120, 2004.

[19] L. Barbé, B. Bayle, M. de Mathelin, A. Gangi, "In Vivo Model Estimation and Haptic Characterization of Needle Insertions", The International Journal of Robotics Research, 26: 1283-1301, 2007.

[20] A. Asadian, M.R. Kermani, R.V. Patel, "A Novel Force Modeling Scheme for Needle Insertion Using Multiple Kalman Filters," Instrumentation and Measurement, IEEE Transactions on , vol.61, no.2, pp.429-438, Feb. 2012

[21] A. Asadian, M.R. Kermani, R.V. Patel, "A compact dynamic force model for needle-tissue interaction," Engineering in Medicine and Biology Society (EMBC), 2010 Annual International Conference of the IEEE , vol., no., pp.2292,2295, Aug. 31 2010-Sept. 4 2010

[22] M. Basseville, I. Nikiforoc, "Detection of Abrupt Changes: Theory and Application", Prentice Hall, 1993.
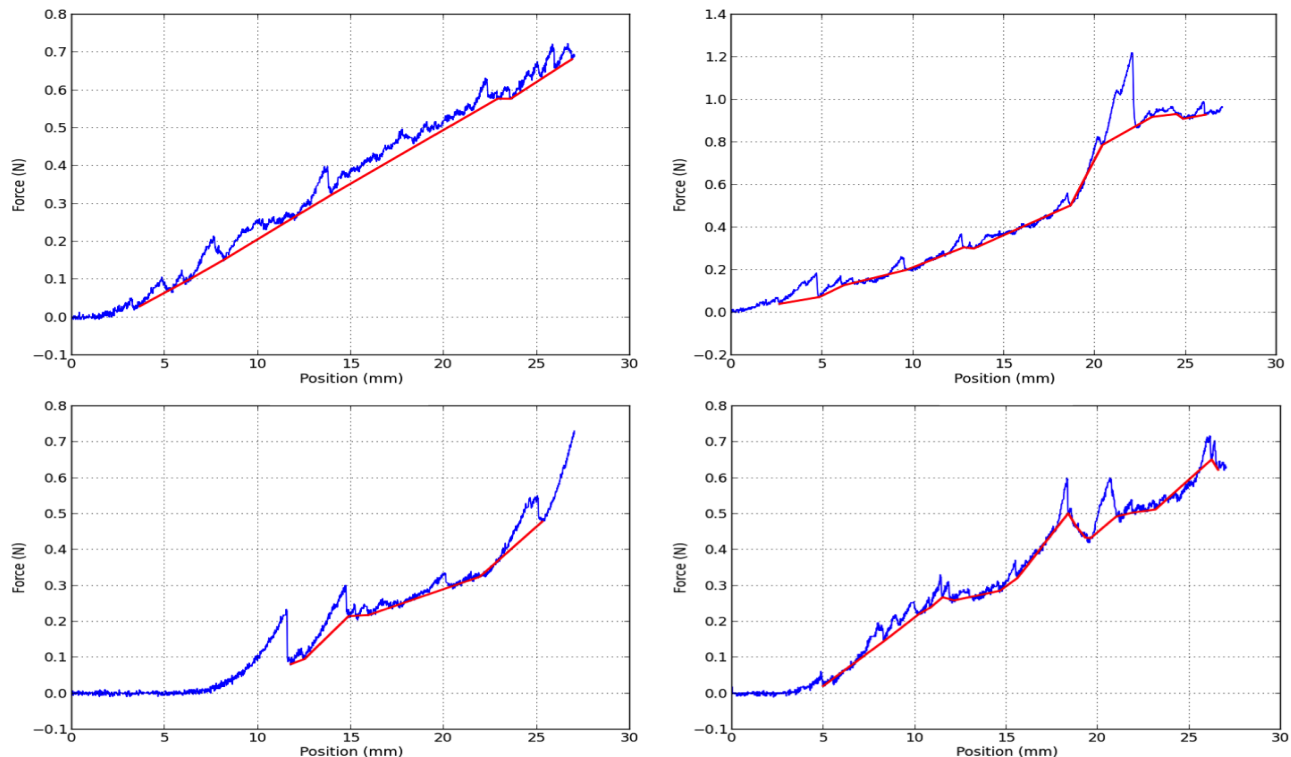
Figure 6 Four examples of friction force with the locally fitted linear model. As can be seen, friction trend follows the different force shapes. Top left: steady cutting with constant friction pattern. Top right: vein puncture patterns are characterized by higher slopes and friction (19 to 22 mm). Bottom left: at 15 mm it can be seen a typical plateau associated with needle-tissue slip. In the top left insertion it can also be observed at approximately 22 mm insertion. Bottom right: from 17 to 20 mm the force acting on the needle decreases. The reasons are not well understood yet.